Oil & Natural Gas Technology

DOE Award No.: DE-FC26-06NT43067

Quarterly Progress Report

(January – March 2008)

Mechanisms Leading to Co-Existence of Gas and Hydrate in Ocean Sediments

Submitted by:
The University of Texas at Austin
1 University Station C0300
Austin, TX 78712-0228

Prepared for:
United States Department of Energy
National Energy Technology Laboratory

May 6, 2008

Office of Fossil Energy

MECHANISMS LEADING TO CO-EXISTENCE OF GAS AND HYDRATE IN OCEAN SEDIMENTS

CONTRACT NO. DE-FC26-06NT43067

QUARTERLY PROGRESS REPORT
Reporting Period: 1 Jan 08 – 31 Mar 08

Prepared by

Steven L. Bryant
Department of Petroleum and Geosystems Engineering
The University of Texas at Austin
1 University Station C0300
Austin, TX 78712-0228
Phone: (512) 471 3250
Email: steven_bryant@mail.utexas.edu

Ruben Juanes
Department of Civil and Environmental Engineering
Massachusetts Institute of Technology
77 Massachusetts Avenue, Room 48-319
Cambridge, MA 02139
Phone: (617)253-7191
Email: juanes@mit.edu

Prepared for
U.S. Department of Energy - NETL
3610 Collins Ferry Road
P.O. Box 880
Morgantown, WV 26508

Summary

Work during this quarter focused on the discrete element modeling (DEM) coupling of fluid flow and sediment mechanics when two fluid phases are present, and on evaluating the coupling of capillarity and grain displacement with a kinematic extension of the previously developed level set method (LSM/PQS).

In previous months, we had developed a robust grain-scale model of the coupling between sediment mechanics and single-phase fluid flow. We have further refined that model so that it has better predictive capabilities of the macroscopic fluid-flow parameters (like intrinsic permeability) and poromechanical parameters (such as the Biot coefficient). But the major development during the first quarter of 2008 has been the implementation of a two-phase flow model in PFC. The coupled model now allows us to investigate the mechanisms of capillary invasion and sediment fracturing using a rigorous micromechanical model.

The kinematic model of grain displacement is not mechanically rigorous but yields useful qualitative insight. On one hand, fracturing a sediment is likely to impede the subsequent drainage of brine from that sediment. On the other hand, the grain displacement lowers the capillary pressure needed for drainage in the direction of the fracture. Thus competition between capillary entry pressure and fracture initiation/propagation pressure may not be limited to the initial event in an unfractured sediment.

A paper for the Offshore Technology Conference to be held in Houston has been completed, and two papers for the International Conference on Gas Hydrates that will take place in Vancouver were completed in April 2008. A paper proposal for the Society of Petroleum Engineers Annual Technical Conference and Exhibition (Sept. 2008) has been accepted.

Activities in This Reporting Period

<u>Task 4.0 – Fracture Initiation and Propagation</u>

<u>Subtask 4.1. Initialize the model</u>

This task has been completed, and reported upon in previous communications.

<u>Subtask 4.2. Poromechanics with a single-fluid system</u>

We have refined our coupled micro-poromechanical model, which now has better predictive capabilities for macroscopic hydraulic properties (like intrinsic permeability of the porous medium).

As an illustration of the validity of the model, we show below the comparison between the numerical results and the analytical solution for a uniaxial fluid flow test. The analysis permits to back out the intrinsic permeability (and its dependence on grain size), and the consolidation coefficient (and its dependence on the fluid bulk modulus and grain stiffness). The results are in agreement with the well established Biot theory of linear poroelasticity.

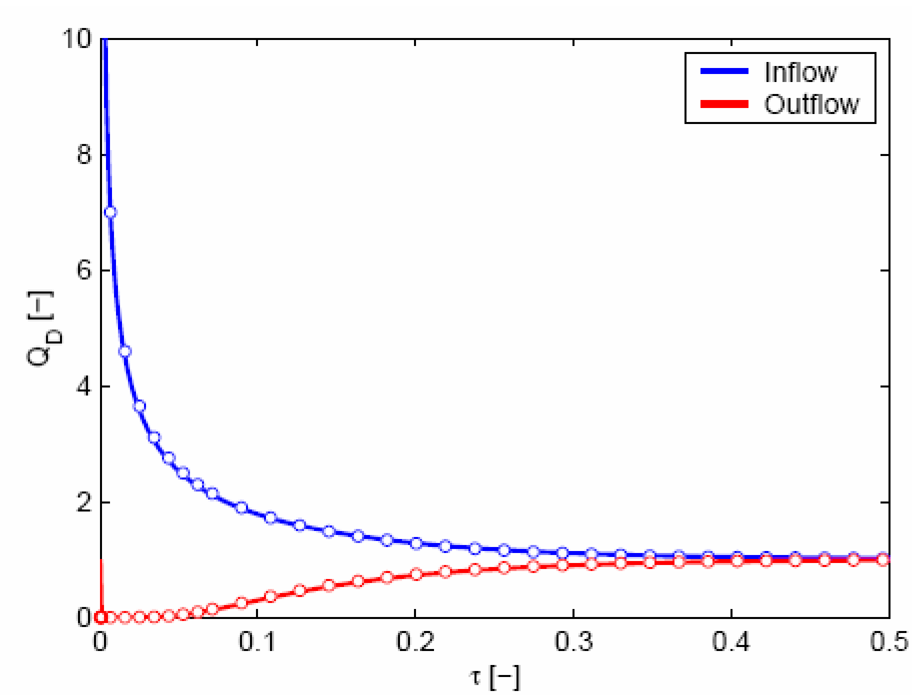

Figure 1. Inflow and outflow rates into the pressure cell during a uniaxial flow test. Comparison of DEM simulation (dotted line) and analytical solution (solid line).

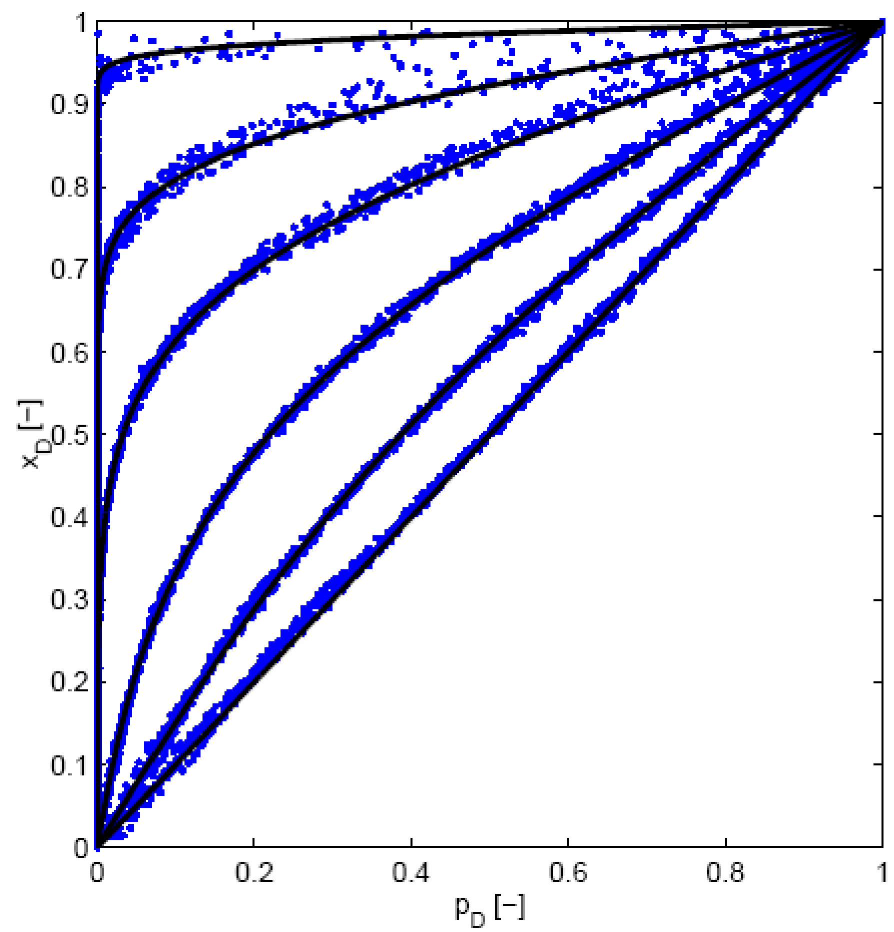

Figure 2. Evolution of pressure profiles during a uniaxial flow test. Comparison of DEM simulation (dotted line) and analytical solution (solid line).

Subtask 4.3. Hydraulic fracturing with an elastic membrane representation of a two-fluid system

In the environments of interest for methane hydrates—in particular, at the base of the hydrate stability zone—two fluid phases exist: a liquid brine phase, and methane gas. One of the key differences between single fluid and two fluid systems is the presence of a fluid-fluid interface. Due to surface tension effects, the pressures on both sides of the interface (that is, the pressure of brine and the pressure of methane gas) can be very different. This pressure difference may lead to preferential fracturing of the sediment (Figure 3). While this is typically not a favored scenario in single-fluid systems, it is natural in two-fluid systems.

Here, we adopt an "elastic membrane" representation of the gas/water interface that only allows normal forces to be transmitted. Adhesion forces are neglected at this stage. When the bond between two grains is lost, the "membrane" advances and a new pore is loaded with a higher pressure. A simple and elegant formulation of the key hydraulic property (the conductance between pore bodies) has recently allowed us to consider such processes. The basis is to allow flow (that is, have a positive conductance between two pores) only when the bond between grains is broken, and a gap of sufficient width has been formed

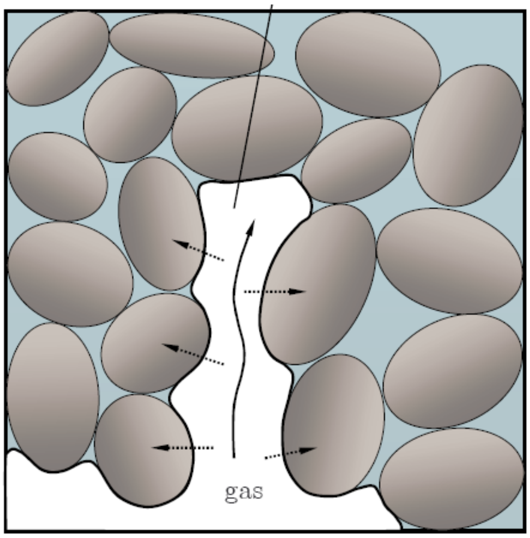

Figure 3. Fracturing of a sediment in a two-fluid system.

These developments permit investigating the poromechanical behavior of model sediments under a variety of scenarios. Of particular interest is the influence of bonding between grains, and the dependence of the mechanical deformation on the strength of those bonds. The model now allows one to investigate under which conditions the material will “fracture” (the fluid pressure is sufficiently high that bonds will break under tension). By resolving the dynamics of the flow and the texture (layering) of the sediment, we can also investigate whether failure will be isotropic or in a preferential direction. While these issues have been investigated at length for dry media, their characterization for fluid-saturated media (especially, when two fluids are present) is still an open issue.

We are particularly interested in the simulation of sediment fracturing upon invasion of a second fluid phase. As explained earlier, we adopt an “elastic membrane” representation of the gas/water interface that only allows normal forces to be transmitted. When the bond between two grains is lost and/or the gap between grains is sufficiently large, the “membrane” advances and a new pore is loaded with a higher pressure. We can model the advancement of the fluid-fluid interface and, correspondingly, the changes in pore pressure. We find that, under many scenarios of interest, this leads to fracturing of the medium. This is shown in Figure 4.

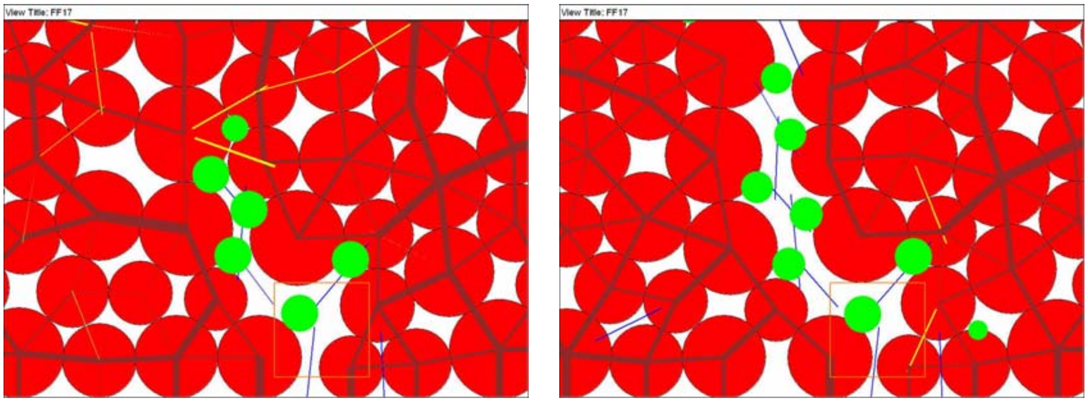

Figure 4. Illustration of fracturing of the sediment due to invasion of a gas phase into a brine-saturated sediment. The green dots represent the pores that have been invaded by gas. Gas and brine pressure are different due to the surface tension effects. This example is representative of the typical behavior observed numerically for the mechanical behavior of granular materials under fluid-fluid displacements.

In many (passive) depositional environments, the horizontal stress is lower than the vertical stress. In such scenarios, one expects the development of vertical fractures that open up the sediment in the direction of minimum compressive stress, and the conceptual picture shown in Figure 4 is relevant. In Figure 5 we show that fracturing of the sediment is not necessarily restricted to anisotropic Earth stresses. Even when horizontal and vertical stresses are equal, the medium tends to fracture in a set of radial, geometrically complex fractures, if gas is injected into a brine-saturated sediment.

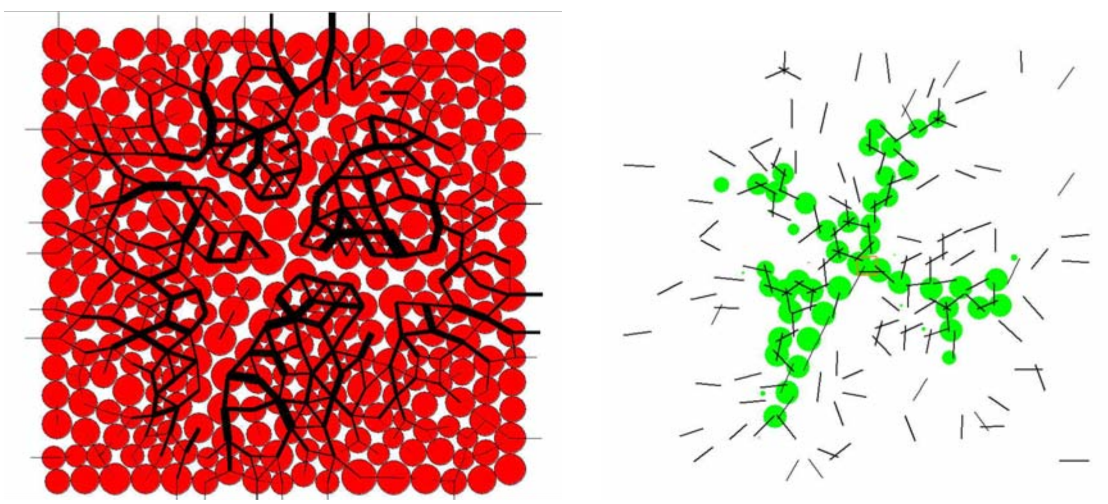

Figure 5. Illustration of the fracturing behavior of a model sediment upon injection of gas, when the vertical and horizontal stresses are equal. The sediment fractures “isotropically” into a set of radial, geometrically-complex fractures.

Noteworthy is the ability of the model to predict which one of the two end-member mechanisms for methane transport (sediment fracturing or capillary invasion) is dominant. We find that the most sensitive factor is the grain size: fracturing is favored for fine-grained sediments, while capillary invasion is favored for coarse-grained sediments. We will report on our theoretical analysis of this competition, as well as on the validation of the coupled grain-scale model, in future communications. In Figure 6 we simply show a snapshot of the mode of methane migration for the two end-member systems.

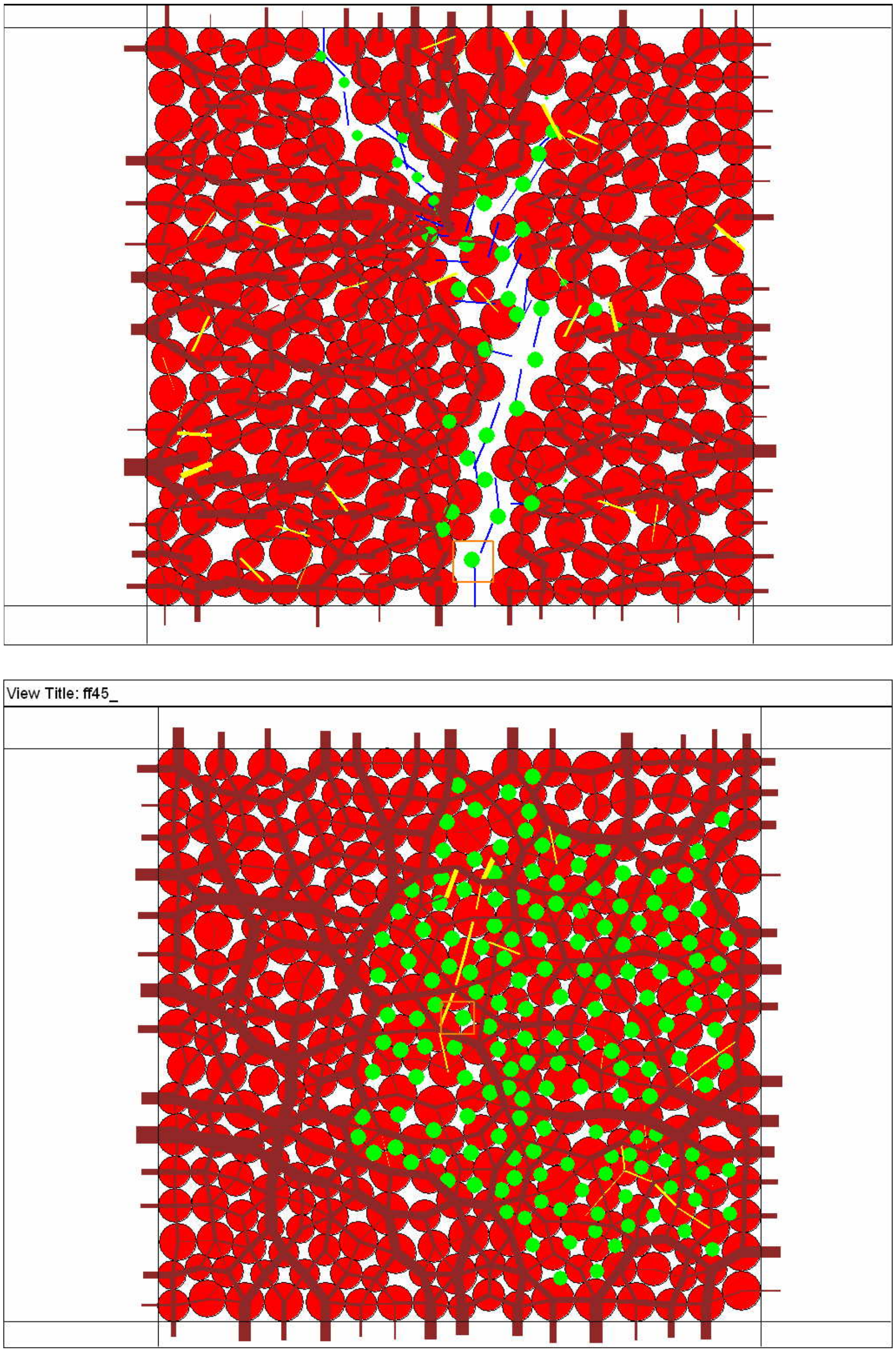

Figure 6. Snapshot of the mode of methane migration for two end-member systems: fine-grained sediment showing vertical fracturing (top), and coarse-grained sediment showing capillary invasion (bottom).

Task 5.0 – Compute Grain-Scale Gas/Water Geometry

As a means of exploring the coupled behavior of meniscus movement and grain movement, we develop an approach complementary to the DEM for grain poromechanics with two fluid phases, with grain mechanics somewhat simplified, but with the advancing fluid-fluid interface computed rigorously. To simulate grain mechanics, we introduce the following steps after each PQS drainage step:

1) Identify grains in contact with non-wetting phase.
2) The non-wetting fluid (gas) exerts force, the vector sum of which we denote $\vec{F}_i$, on each grain *i* identified in step 1. Per the elastic membrane model, locally the force is normal to the fluid-grain contact (see Figure 5.1). To obtain $\vec{F}_i$, we integrate the normal vector $\vec{n}$ (pointing outwards from the gas phase) along the part Γ_{Gi} of the entire grain perimeter (surface) Γ_i in contact with gas. The then find the unit vector $\vec{f}_i$ in the same direction as $\vec{F}_i$.
3) Compute a displacement $\vec{s}_i$ in response to the force computed in step 2. The force is maximum when Γ_{Gi} is half-circle (half-sphere) so we set $\vec{s}_i = 4r(1-r)C\vec{f}_i$, where *r* is ratio of the lengths (areas) of Γ_{Gi} and of entire Γ_i, and *C* is a pre-set constant.
4) The center of grain i moves by $\vec{s}_i$ determined in step 3, but only if it will not overlap substantially with any other grains in its new position. By “substantially” in this work we mean that the distance between the grain centers would be less than 0.8 of the sum of their respective radii.

This conceptual procedure does not consider the forces imposed by neighboring grains, which are the essence of the solid mechanics; this is the proper role of DEM described above. Thus we do not attempt to determine the exact magnitude of F_i, nor the exact displacement $\vec{s}_i$ from Newton’s 2nd law. The kinematic approach simply provides insight into the type of behavior that can arise from the coupled displacements.

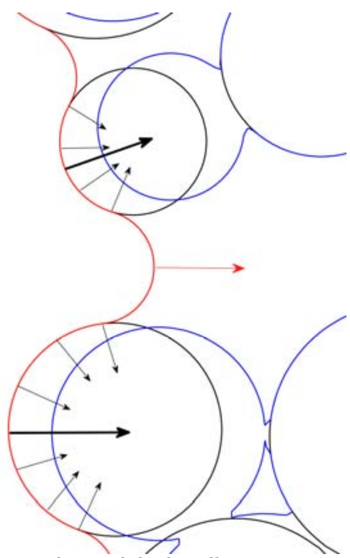

Figure 7. Schematic of a kinematic model of sediment movement driven by capillary pressure difference. Non-wetting fluid interface is shown in red and the initial grain position is shown in black. Small black arrows show the normal vectors along the contact line between non-wetting fluid and grain surface. Enlarged black arrows show their (integral) direction and consequently the direction of grain movement. New grain positions are outlined in blue.

Level Set Method/Progressive Quasistatic Algorithm (LSM/PQS) Results for Drainage Coupled with Grain Displacement

We have previously described the development of the LSM and the PQS for capillarity controlled displacements. It was straightforward to extend the algorithm to include kinematic grain motion as described above. Here we illustrate the coupled behavior in two 2D packs of circular grains. The first one was obtained by packing disks of unit radius on a regular triangular grid except for one disk that was slightly offset (see Figure 8). Drainage curves (Figure 9) show remarkable qualitative and quantitative differences for this simple medium due to coupling of fluid and sediment movement. In the case of stationary grains (not shown), almost all the pore throats are the same size and thus almost the entire domain drains quite suddenly when the applied curvature increases to 11. When fluid pressure displaces the grains, Fig. 8, the domain begins to drain at much smaller curvatures, the percolation threshold is much less sharp, and the irreducible wetting saturation is larger. The first of these three observations makes intuitive sense: moving grains apart decreases the critical curvature required to force a meniscus between them. Less obvious are the second and third observations. Behind the advancing gas phase, grains are pushed into each other, narrowing the pore throats between them. This increases the pressure required to invade the undrained region behind the leading edge of the advancing front. Thus the drainage curve is smoothed out in the coupled displacement.

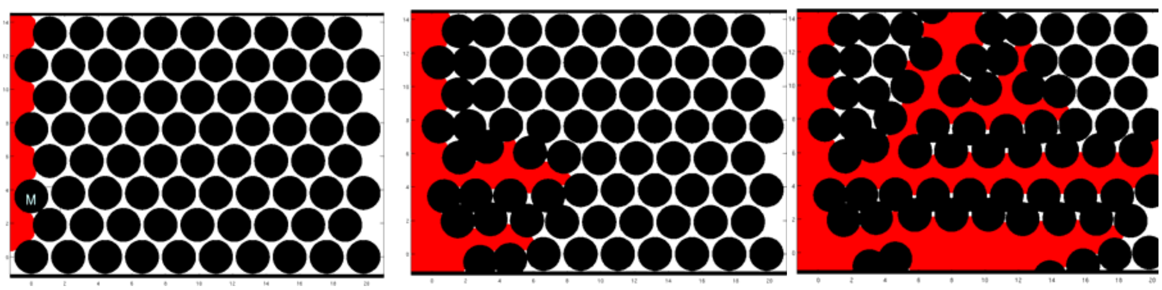

Figure 8. (Left) NW fluid at the first step of PQS simulation is shown in red, C=2.36. The discs (in black) form a regular packing except for one disk in the first column, marked by letter M, that is offset slightly. moved yet. (Center) NW fluid at C=6.36 of the coupled PQS simulation. The packing "irregularity" has, under coupled fluid and sediment movement, triggered an opening of two fluid pathways. (Right) Fluid/sediment configuration at the point where NW fluid percolates to the other side (C=8.56).

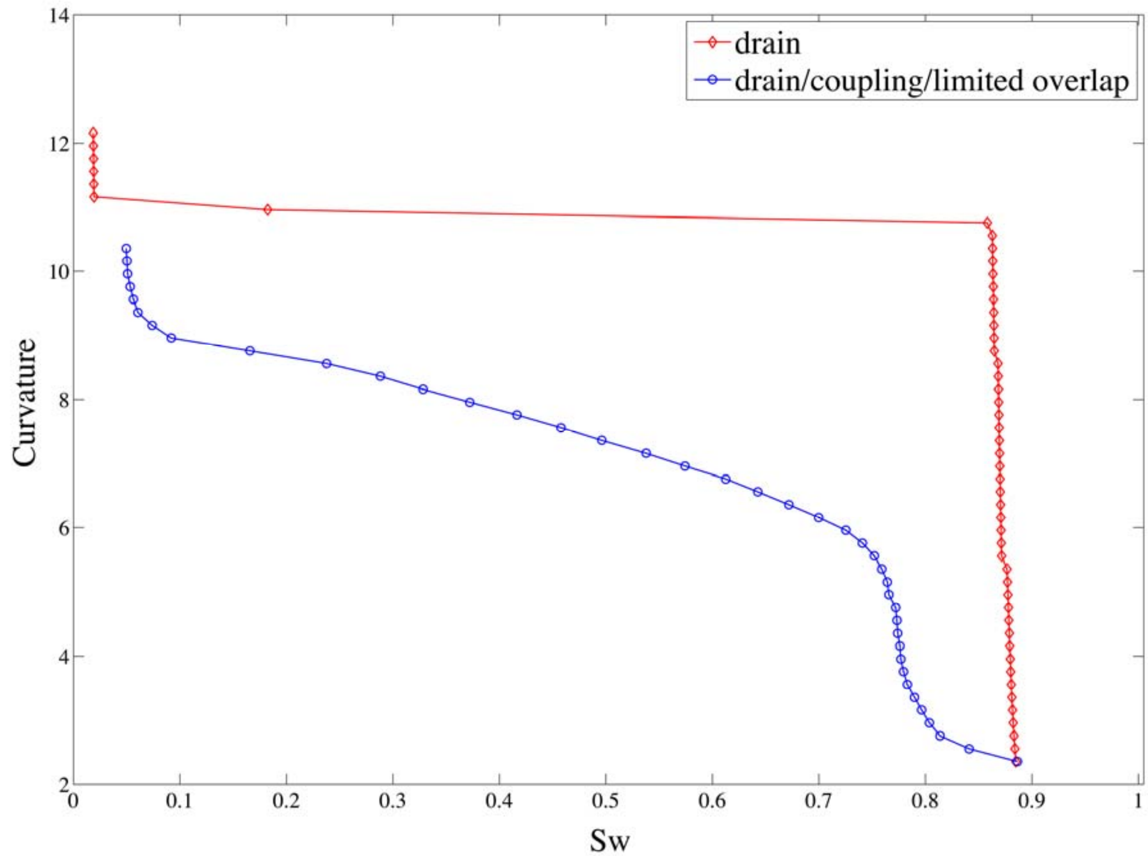

Figure 9. Comparison of curvature-wetting fluid saturation curves for drainage in the regular packing of disks with and without coupling. Note that the initial packing has basically only two throat sizes. Thus if the grains are stationary, once curvature is high enough to drain the smaller throats, the whole rest of the domain drains. This yields a characteristic single large jump in the corresponding C-Sw curve.

The second geometry is a 2D cross-section of a dense, random packing of equal spheres. This yields a packing of disks with radius 1 or less (Figures 10 and 11). We removed three disks at the entrance to create a preferred region for onset of grain displacement. The displacement becomes self reinforcing: moving a grain decreases the curvature required for drainage to occur, leading to gas invasion that moves grains apart in the invaded pore.

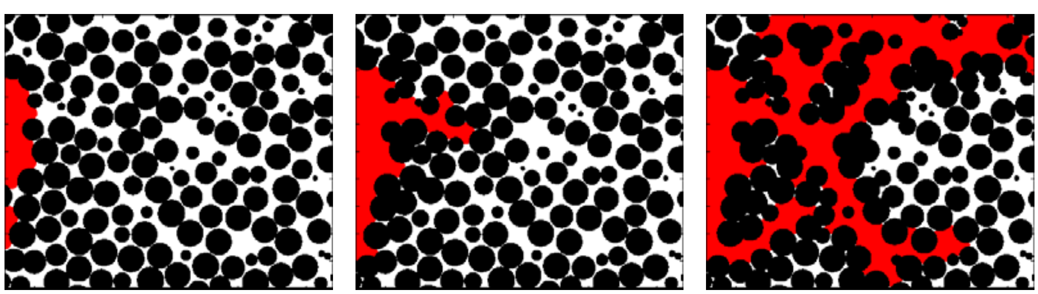

Figure 10. (Left) NW fluid at the first step of PQS simulation is shown in red (C=2.48). The discs (in black) have not moved yet. (Center) NW fluid at C=3.68 of the coupled PQS simulation. The fluid has opened a pathway, which just started to split into two. (Right) Fluid/sediment configuration at C=6.08 where NW fluid percolates to the other side for the first time.

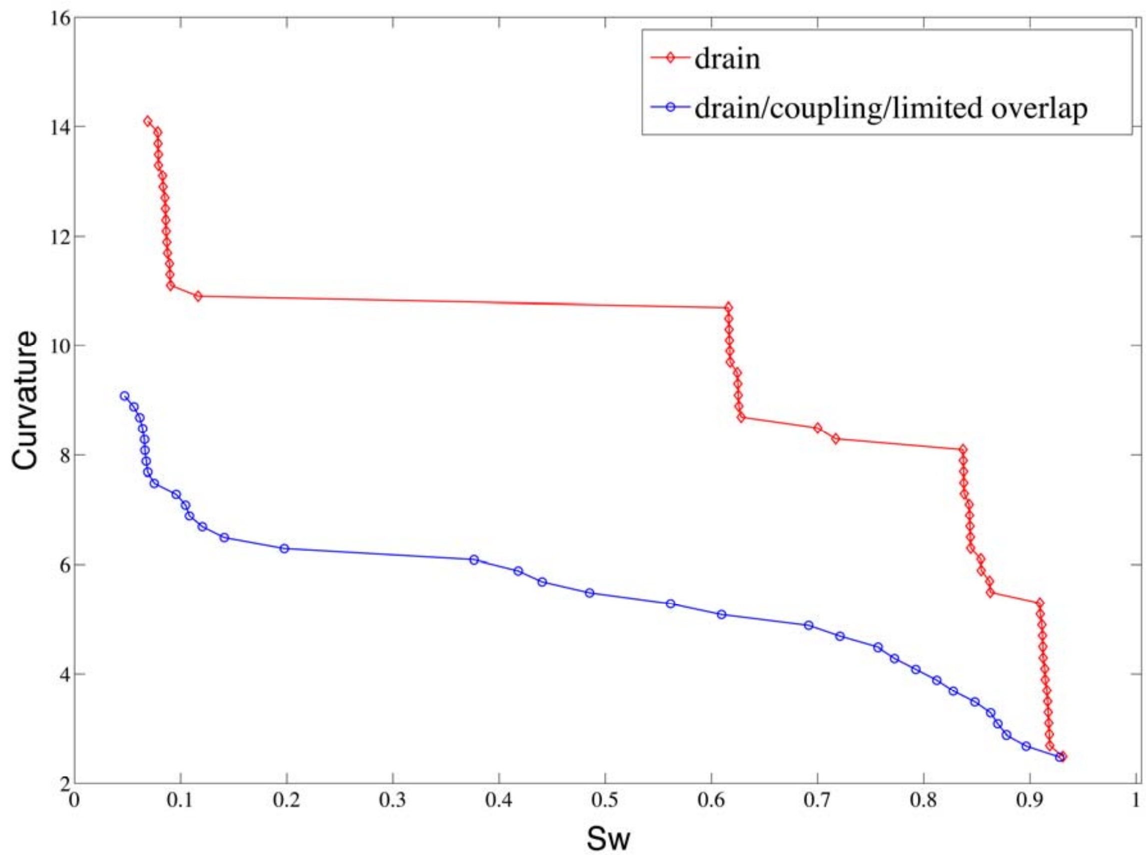

Figure 11. Comparison of curvature-wetting fluid saturation curves for drainage in the regular packing of disks with and without coupling.

The coupling implemented above is not physically rigorous. Nevertheless it shows that the fluid and granular movement can be successfully put together. Moreover the qualitative similarity of the invaded region in Fig. 10 (rigorous capillarity with nonrigorous grain movement) and in Fig. 6 (rigorous grain mechanics with nonrigorous capillarity) is remarkable. We are thus optimistic that these models are capturing important features of the coupled system. Importantly for this application, the physical character of the drainage displacement changes when grains move. Coupling with the physically correct granular movement (simulated via DEM) will be slightly more involved (due to different software/platforms) and is part of the future work.

National Energy Technology Laboratory

626 Cochrans Mill Road
P.O. Box 10940
Pittsburgh, PA 15236-0940

3610 Collins Ferry Road
P.O. Box 880
Morgantown, WV 26507-0880

One West Third Street, Suite 1400
Tulsa, OK 74103-3519

1450 Queen Avenue SW
Albany, OR 97321-2198

2175 University Ave. South
Suite 201
Fairbanks, AK 99709

Visit the NETL website at:
www.netl.doe.gov

Customer Service:
1-800-553-7681